Proceeding of the 15th ME-NETT Conference

Study of Turbulence and Cycle-to-Cycle Variation Levels in SI Engine Cylinders

P ASADAMONGKON*, N St HILL, K C LEE, and M YIANNESKIS
Department of Mechanical Engineering , King' S College, UK
*Department of Mechanical Engineering , Faculty of Engineering , Srinakharinwirot University
Phone 66(2)6641000 Ext 2063, E-mail :Pichaias@psm.swu.ac.th

ABSTRACT

This paper describes an experimental investigation of the cycle-to-cycle (Cyclic)variations and instability of the jet flows in the cylinders of the dual-intake valves gasoline engines under both steady-state and motored engine condition using Laser-Doppler anemometry and spectral analysis techniques. The instability of the jet flows around the inlet jet valves was studied under steady state condition. Cyclic variations observed near the centre of the cylinder were investigated by comparing turbulence and cycle-to-cycle variation levels within the region to those found within the intake jet of the motored engine. Spectral analysis techniques were also used to study velocity spectra at these locations. The results show that cyclic variations broaden the true turbulence levels substantially and should be taken into account when assessing the turbulent flow processes and related predictions.

INTRODUCTION

The pre-combustion flowfield and turbulence levels in SI engines affect flame propagation and performance. Accurate quantification of the amount of turbulence present in the combustion chamber before TDC of compression is therefore necessary.

For this purpose determination of cyclic variation and flow instabilities that may broaden the measured turbulence levels is essential. Findings of recent studies by others suggest that there are a number of factors which may influence turbulence levels in engines. Studies of the flows within motored engines have suggested swirl centre precession and cycle-to-cycle variation as probable causes [1,2]. Instabilities were found to occur even under steady flow conditions, and the presence of vortex breakdown [3] and vortex shedding [4] have been suggested. Instability under the intake ports of a dual-intake valves gasoline engine, often termed jet flapping, can be studied under motored engine conditions by quantifying the cycle-resolved turbulence and cycle-to-cycle variation at individual points within the cylinder. A number of techniques have been employed for quantification and analysis of cycle-resolved and cycle-to-cycle variation levels [5,6,7].

Most studies of the flow in Spark Ignition (SI) engines have concentrated on the in-cylinder flow due to the difficulties associated with the application of non-obtrusive optical techniques to complex geometries such as those of the inlet port. These problems may be overcome by using a refractive index matching technique in combination with laser-Doppler anemometry (LDA) [8].

In the present work LDA and refractive index matching techniques are used to study instabilities within the inlet jet under steady flow conditions by determining the values of skewness and kurtosis of the probability distribution function (PDF) of the instantaneous velocities. LDA is also used in combination with spectral analysis to study the flow within a motored engine cylinder with a transparent Pyrex cylinder.

EXPERIMENTAL SETUP

The major features of the motored engine and steady flow replica are shown in Figure 1, with the geometric specifications listed in Table 1. A schematic diagram of the LDA optical system is given in Figure 2. Both cylinder head have directed inlet ports and pent-roof combustion chambers. The co-ordinate system employed is also shown in Figure1.

Table 1 Geometrical specifications of Ford Zetec and Cosworth dual-intake Valves

Engine design	**Ford Zetec**	**Cosworth**
Experimental rig	Motored	Steady Flow
Bore (mm)	80.6	86
Port angle β (°)	65.8	57
Angle between ports γ (°)	16	16
Inlet valve diameter DV(mm)	32	35
Inlet valve angle α (°)	20	17
Maximum valve lift (mm)	9.3	9.00
Dxx (mm)	16.8	16.5
Dyy (mm)	19.3	17.6

Motored optical engine

The engine was a single cylinder engine equipped with the four-valve cylinder head of a 1.8 litre Ford Zetec engine cylinder head seated on a pyrex glass cylinder, and driven by an electric motor. Most of the asurements, including these reported here, were at 500 rpm; extensive tests at different speeds nd 1000 rpm) were made to establish scaling of with engine speed. The experiments were l in the motored engined described in detail in [1. ain engine characteristics are list in Table 2.

Table 2 Operating characteristics of motored engine

Displacement	1796 cc
Bore	80 mm
Stroke	90 mm
Compression Ration	10:1
Inlet Valve diameter	32 mm
Exhaust Valve diameter	28 mm

The Pyrex glass cylinder allowed optical access throughout the cylinder. The working fluid was air seeded with silicon particles. The engine speeded was monitored by a shaft encoder attached to the crankshaft, which produced 1000 pulse/rev of crankshaft. An optical interrupter mounted on the cam was used to indicate TDC of the induction stroke. The encoder pulses were fed to a Burst Spectrum Analyser (BSA) and used to check the arrival of data. In-cylinder pressure was monitored by means of a Kistler pressure transducer, which was mounted in the position of the spark plug so that the tip was flush with the top of the pent-roof.

Steady Flow rig

The Cosworth engine port, cylinder and valve were manufactured from a clear cast acrylic (Perspex) block in a CNC machine. The valves were manufactured from Perspex rods. The experiments were performed in steady flow rig described in detail in [9]. In order to ensure accurate matching of the refractive indices of the fluid and acrylic material, the temperature of the fluid mixture was controlled by a proportional temperature control system and kept constant to within ±0.5°C during the experiments. Heating and cooling coil was inserted into the fluid tank and was connected to the temperature control system. The working fluid was a mixture of oil of turpentine and tetraline in the volume ratio of 69.2:32.8, which has an identical refractive index to that of Perspex at 24 °C. Artificial seeding was not necessary because natural contaminants in the fluid provided a sufficient

number of scattering particles. The experiments were carried out with both valves set at 9mm lift, with a liquid mass flow rate of 3.06 kg/s, corresponding to a Reynolds number, based on the hydraulic diameter of the inlet port, of 60,753. The geometrical similarities of the motored engine and steady flow geometries allow comparisons of the flows to be made, but clearly shape differences may have important influences and such comparisons must be made with care.

Measurement technique

The principal characteristics of the LDA systems used are listed in Table 3 and a schematic diagram of their optical arrangement is shown in Figure 2. Both LDA systems were operated in the forward scatter dual-beam mode. A diffraction grating was used to split the laser beam as well as provide the appropriate frequency shift between the two first order beams. Instantaneous velocity signals were measured using the BSA (Dantec, model 57N21 master). The quality of the Doppler signals were monitored continuously on an oscilloscope and the data and validation rates were monitored online, on the computer screen. Arrival rates as high as 40 kHz were obtained in the motored engine rig, and this was found to be sufficient to determine time-resolved turbulence levels during individual engine cycles. For the steady flow, data were obtained from 10,000 validated samples at a data rate of approximately 8.5 kHz.

Table 3 Principal characteristics of the laser Doppler anemometry systems

Experimental rig	Steady Flow	Motored
Laser	He-Ne	Argon-ion
Wavelength, X (nm)	632.8	514.5
Power (mW)	10	1000
Expanded beam diameter (at e'2 intensity)	0.83	0.83
Half-angle between incident beams(°)	4.27	5.98
Intersection volume diameter (at e^2 intensity), (μm)	77	120
Intersection volume length (at e^2 intensity), (μm)	1043	1140
Stationary fringes within the e 2 intensity level	19	48
Frequency to velocity conversion factor (m/s/MHz)	4.3	2.47
Frequency shift (MHz)	3.6	2.47

Motored engine data treatment

The mean velocity, turbulence and cycle-to-cycle variation characteristics are of particular relevance for the initiation of combustion and flame kernel growth. The turbulent and unsteady velocity field in an internal combustion engine is characterised by cycle-to-cycle variations at low frequencies, which increase the velocity fluctuations. Different techniques have been proposed (see, for example, [6], [10]) for the determination of the turbulence levels by the removal of the low frequency components.

In this work, the data was processed using a low pass filter, to differentiate between cyclic variation and turbulence following a similar principle as employed in [7]. The relationships used to quantify the values of ensemble mean velocities, turbulence levels and cycle-to-cycle variations are described below to clarify the terms employed. The ensemble-averaged angle-resolved mean velocity of N valid cycles at crank angle θ is given by:

$$\langle U(\theta)\rangle = \frac{1}{N_v}\sum_{i=1}^{N} U(\theta,i) \qquad (1)$$

where N_y (θ) is the total number of valid velocity estimates at crank angle interval θover all N cycles, for each cycle i and

$$U(\theta,i) = \langle U(\theta)\rangle + u(\theta,i) \quad (2)$$

where $U(\theta,i)$ is the instantaneous velocity and $u(\theta,i)$ is the fluctuating velocity. On filtering, the fluctuating velocity may be separated into low and high frequency components:

$$U(\theta,i) = \langle U(\theta)\rangle + u_{LF}(\theta,i) + u_{HF}(\theta,i) \quad (3)$$

The filtered in-cycle mean velocity is the sum of the ensemble-averaged mean and the low frequency fluctuation:

$$U_{LF}(\theta,i) = \langle U(\theta)\rangle + u_{LF}(\theta,i) \quad . \quad (4)$$

$$\langle U_{LF}\rangle = \langle U\rangle \quad (5)$$

The intensities of the high and low frequency fluctuations can be characterised by their variances about appropriate mean velocities.

$$u_{HF} = \sqrt{\langle u_{HF}^2\rangle} = \sqrt{\langle (U - U_{LF})^2\rangle} \quad (6)$$

$$u_{LF} = \sqrt{\langle u_{LF}^2\rangle} = \sqrt{\langle (U_{LF} - \langle U\rangle)^2\rangle} \quad (7)$$

The ensemble-averaged rms fluctuation intensity u' is related to the low and high frequency fluctuations by

$$u' = \sqrt{\langle (u_{LF} + u_{HF})^2\rangle} \quad (8)$$

where u'_{HF} is referred to as the turbulence level, and u'_{LF} is referred to as the cyclic variation of the mean. The instantaneous velocity for each cycle is lowpass filtered using a Hamming filter with a cut-off frequency of 250 Hz, and a sampling frequency of 16.6 kHz. A similar criterion to that used by [5] is used for selection for the cut-off frequency. Instantaneous velocity fluctuations which were higher than three times the rms fluctuations were discarded. Mean velocity turbulence levels and cycle-to-cycle variation levels were calculated with sample sets where at least 95% of the data were within the $\pm 3\sigma$ a range.

RESULTS AND DISCUSSION

Motored engine

Ensemble-averaged rms, cycle-resolved turbulence and cycle-to-cycle variation

The variations of the axial (in the z-direction) ensemble-averaged filtered and unfiltered mean velocities, the ensemble-averaged rms(w'), the cycle-resolved turbulence (w'_{HF}) and cycle-to-cycle variation (w'_{LF}) with crank angle during induction and compression are presented in Figure 3. Results are shown at one point near the centre of the cylinder (Figure 3(a)) and one within the inlet jet (Figure 3(b)). All motored engine results are normalised with the mean piston speed V_p. Turbulence levels (both w'_{LF} and w'_{HF}} are higher during induction within the intake jet region, as might be expected. Cyclic variation levels are substantial in both cases, but more significant near the centre of the cylinder. In general the w'_{LF} variation with crank angle was found to be similar throughout the cylinder. During compression the w', w'_{HF} and w'_{LF} levels decrease and remain fairly constant. It is clear from Figure 3 that the w' levels may overestimate the amount of 'true' turbulence w'_{LF} by as much as 100% in many pans of the cycle. Measurements of the axial velocity and turbulence level under both valves and along the centre line of the cylinder; and the velocity and turbulence level in the y-direction in the centre plane were also made to characterise swirl levels. They all exhibit the similar features of cyclic variation levels.

Spectral analysis

Figure 4 presents the w-velocity spectra at the same points as in Figure 3, x = 10 and
x = 30 mm. The six most significant peaks are indicated, and found to be multiples of the cam speed of 4.16 Hz, which may suggest that they are harmonics of the cam frequency. Figure 4(a), which represents the velocity spectra at a point near the centre of the cylinder (x = 10 mm), is found to contain a broader band of significant peaks, than within the jet in Figure 4(b). The significant peaks within the broader range are still found to be multiples of the cam frequency, thus suggesting a connection. It may therefore be inferred from the spectra that the cycle-to-cycle variation may be influenced by the engine speed, but that its characteristic frequencies lie within a higher range than might be attributed to the mean flow.

Steady flow tests

In view of the aforementioned high w'_{LF} levels, it is important to understand the origin(s) of such variations, in order to identify means for their control and to predict engine performance better. This is a very complex task, but inlet jet flapping or flow instability may be one such possible source of variation [8]. For this reason, measurements of the predominant (V, in the.(x-direction) velocity component were made under steady flow conditions within the intake jet. Useful indications of possible jet instability are the third and the fourth moment of the velocity probability distribution function (PDF) [11]; these were calculated from the data and skewness (S, normalised by σ^3) and kurtosis (K, normalised by σ^4) profiles are shown in Figure 5. Gaussian distributions have S and K values of 0 and 3 respectively: deviation from such values might imply jet flapping /instability [8]. This is indeed the case in the data of Figure 5: maximum K and S value of 6.9 and -1.7 are observed near the edge of the jet. These indicate that the velocities are intermittently changed in magnitude, which is consistent with the presence of jet flapping. The structure of the inlet jet from with both valves having equal lift of 9.00 mm is shown in Figure 6. The flapping of the inlet jet (as indicated with dabble end arrows) was observed in the video recording. Spectral analysis of the steady flow velocity data also indicated a number of peaks, similar to those in Figure 4, which might also point to flow instability [8].

CONCLUDING REMARKS

The data presented above show clearly that cyclic variation (due to the variation of the mean velocity from one cycle to the next) may be substantial in reciprocating engines; they can result in an overestimation of true turbulence levels by as much as 100% and must be taken into consideration when assessing engine turbulence levels and related CFD predictions. The origins of such high variations are not clearly understood, but analysis of steady flow data suggests that intake jet flapping may be one possible source. The complexity of the 3-D turbulence processes in engines makes identification of these origins a most challenging task, but work is in progress to obtain more extensive data and analysis their spectral content in more detail so as to improve understanding and help improve combustion and engine performance.

REFERENCES

1) **Arcoumanis, C., Hadjiapostolou, A. and Whitelaw, J. H.,** "Swirl center precession in engine flows", SAE paper 870370, 1987.

2) **Suen, K. 0.,** "Investigation of gas flow in a motored high speed diesel engine by Laser-Doppler anemometry", Ph.D. thesis. University of London, King College, 1992.

3) **Coghe, A., Brunelo, G., and Tassi, E.,** "Effect of intake ports on the in-cylinder air motion under steady flow conditions", SAE paper 88034, 1988.

4) **Hommersom, G., Evers, D. J. W. M. and Huigen, G.,** "Swirl generation by a directed inlet port of a diesel

automotive engine under steady flow conditions", 3rd Int. Conf. On laser anemometry: advances and applications. University College of Swansea, 26-29 September, pp. 23.1-23.15, 1989.

5) **Liou T.-M. and Santavicca D.A.,** "Cycle resolved LDV measurements in a motored IC engine", Journal of Fluids Engineering, vol 107, 1985

6) **Le Coz J.F.,** "Cycle to cycle correlation between flow field and combustion initiation in an S.I. engine", SAE 920517, 1992

7) **Fansler T.D. and French D.T.,** "Cycle-resolved laser-velocimetry measurements in a reentrant-bowl-in-piston engine", SAE 880377, 1988

8) **Nadarajah, S., Balabani, S., Tindal, M. J. and Yianneskis, M.,** "The turbulence structure of the annular non-swirling flow past an axisymmetric poppet valve", Proc. Instn Mech. Engrs, Part C, Journal of Mechanical Engineering Science, 212 (C6), 455-471, 1998.

9) **Asadamongkon, P.,** "Characteristics of the flow through dual-intake valve gasoline engines", Ph.D. Thesis, King's College London, University of London, 2001.

10) **Baby X. and Floch A.,** "Investigation of the in-cylinder tumble motion in a multi-valve engine: Effect of the piston shape", SAE 971643, 1997

11) **Tennekes, H. and Lumley, J.L.,** A first Course in Turbulence. M.I.T. Press, Cambridge, Mass, 1972.

12) **St. Hill, N.,** "A study of turbulence and cyclic variations levels in internal combustion engine cylinder" , Ph.D. Thesis, King's College London, University of London, 2001.

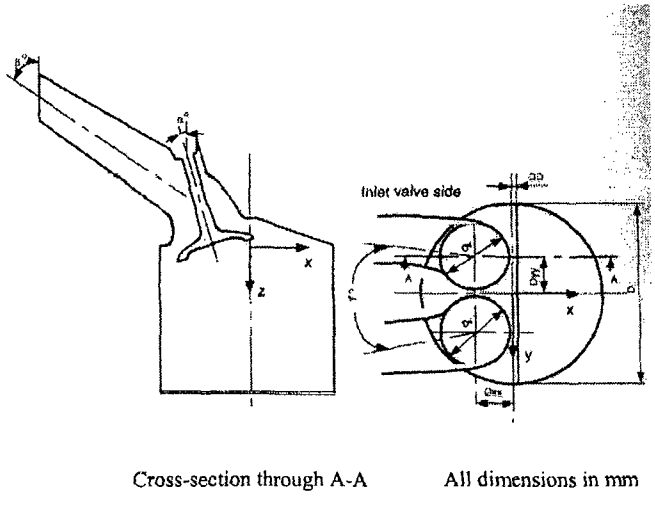

Figure 1 Plane view of engine inlet port and Cylinder geometries.

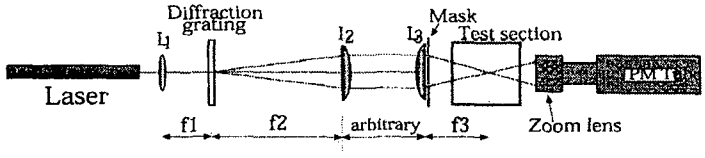

Figure 2 LDA optical systems

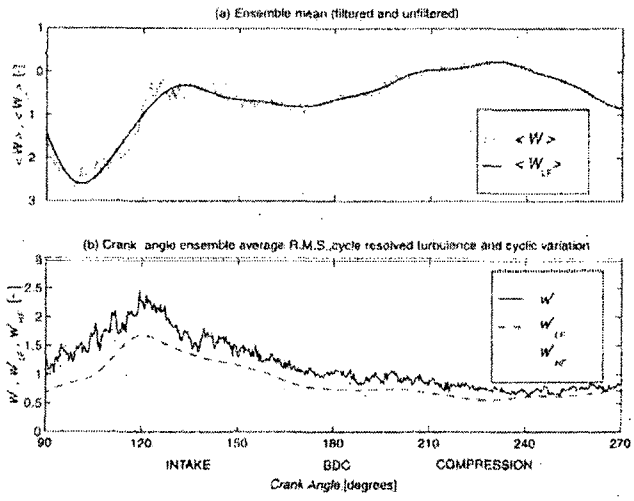

Figure 3(a) Motored engine results at x = 10 mm, y = -17.6 mm and z = 10 mm.

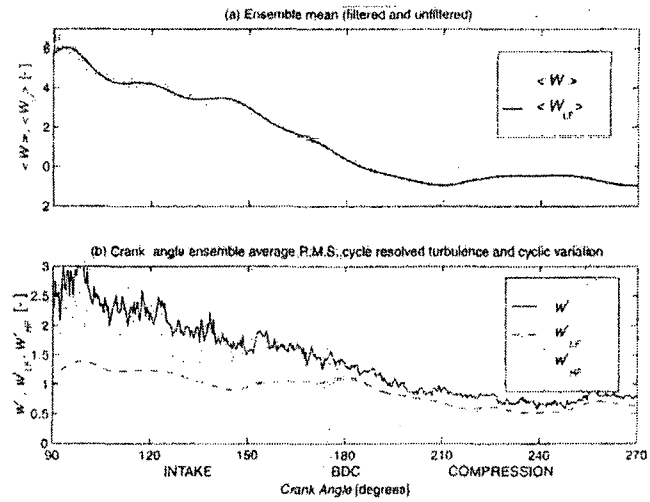

Figure 3 (b) Motored engine results at x = 30 mm, y = -17.6 mm and z = 30 mm.

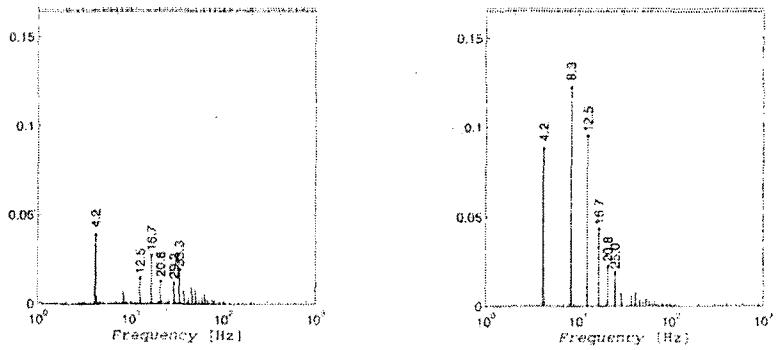

Figure 4 Normalised power spectra at **(a)** x = 10 mm, **(b)** x = 30 mm, y = -17.6 mm and z = 30 mm

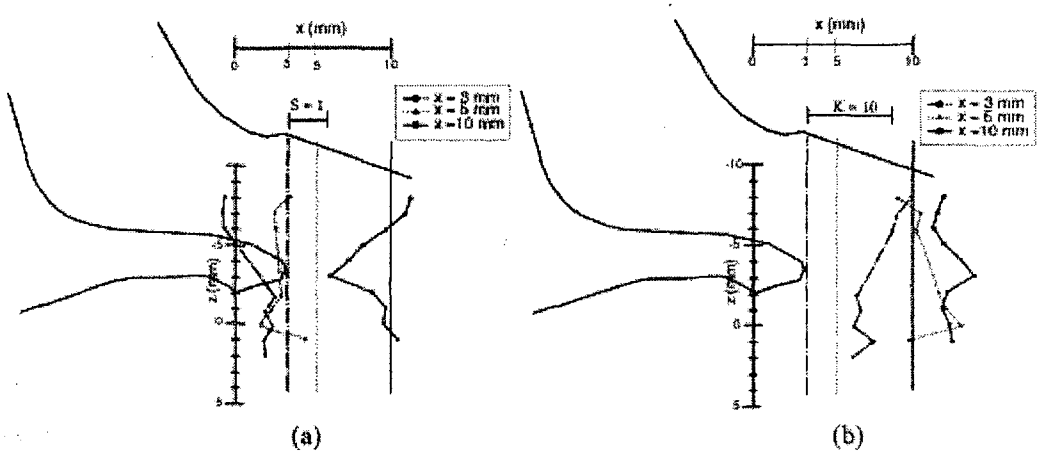

Figure 5 Skewness profiles (a) and Kurtosis profiles (b) in the vertical plane y = -19.3 mm with both valves at 9.00 mm lift.

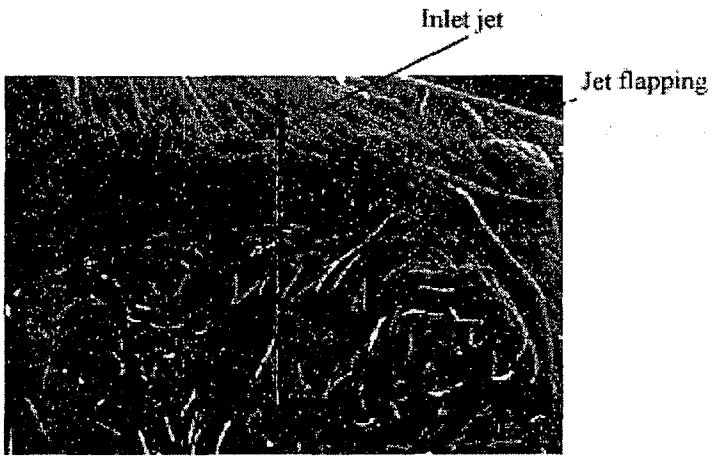

Figure 6 Flow visualisation in the plane y = -19.3 mm.